

# ФІЗИКО-МАТЕМАТИЧНІ НАУКИ

DOI: <https://doi.org/10.32839/2304-5809/2020-6-82-36>

UDC 536.4

Szymon Świontek

Faculty of Materials Science and Ceramics,  
AGH University of Science and Technology

## AB INITIO STUDY OF THERMODYNAMIC PROPERTIES OF THE HEXAGONAL $Ti_6Si_2B$ INTERMETALLIC PHASE

**Summary.** In this paper first principles quantum mechanical approach was used to calculate ab initio thermodynamic properties of  $Ti_6Si_2B$  intermetallic phase. To optimize the geometry of the unit cell appropriate potentials which describe each atom of  $Ti_6Si_2B$  – phase were applied with the use of VASP simulation package. Moreover, the effect of phonon excitations on the lattice parameters, bulk and shear moduli is studied. The results show that  $Ti_6Si_2B$  phase tends to be brittle due to  $B_R/G_R < 1.75$ . However, the thermal expansion coefficients along with a-axis and b-axis change similarly what suggests that investigated phase is thermally stable. Based on free energy calculation the temperature dependences of various quantities such as the lattice constants, thermal expansivity and isobaric heat capacity were reported. Theoretical results were compared with the available experimental data and other ab initio calculations. As a result, it has been proved that  $Ti_6Si_2B$  phase might be considered as high temperature material.

**Keywords:** ab initio study, DFT calculations, VASP approximation, intermetallic phase, high temperature structural applications.

Szymon Świontek

Факультет матеріалознавства та кераміки,  
AGH Університет науки і техніки

## ДОСЛІДЖЕННЯ АВ ІНІТІО ТЕРМОДИНАМІЧНИХ ВЛАСТИВОСТЕЙ ІНТЕРМЕТАЛІЧНОЇ ФАЗИ $Ti_6Si_2B$

**Анотація.** У цій роботі першими принципами був використаний квантово-механічний підхід для обчислення термодинамічних властивостей інтерметалічної фази  $Ti_6Si_2B$ . У літературі доступні лише обмежені дані про фазові рівноваги. Більшість експериментальних відомостей стосуються розрахованих ізотермічних ділянок. У цій роботі, в рамках досліджень пов'язаних із системами  $Ti-Si-B$ , я представляю результати присвячені атермодинамічним властивостям  $Ti_6Si_2B$ . Для оптимізації геометрії одиничної комірки були застосовані відповідні потенціали, які описують кожен атом  $Ti_6Si_2B$  – фази з використанням пакету моделювання VASP. Крім того, вивчається вплив збудження фотонів на параметри решітки, об'ємні та зсувні модулі. Потім, використовуючи формалізм параметрів Грюнезена, було визначено значення коефіцієнта лінійного теплового розширення – як функції температури. Результати показують, що фаза  $Ti_6Si_2B$ , як правило, крихка завдяки  $B_R/G_R < 1.75$ . Однак, коефіцієнти теплового розширення разом із віссю a і b змінюються аналогічно, що говорить про те, що досліджувана фаза є термічно стабільною. Фаза, яка має найменше значення енергії пласта, є кращою у конкретній складовій системі. На основі розрахунку вільної енергії повідомлялося про температурні залежності різних величин, таких як постійні решітки, теплова розширеність та ізобарна теплоємність. Теоретичні результати порівнювались з наявними експериментальними даними та іншими обчислювальними методами. В результаті було доведено, що фаза  $Ti_6Si_2B$  може розглядатися як високотемпературний матеріал. Ця фаза вважається високотемпературним структурним застосуванням через їх феноменальні фізичні, механічні та хімічні властивості. Було доведено, що  $Ti_6Si_2B$  поводяться природним шляхом, демонструючи позитивне значення LTEC у всіх температурних межах від 0 К до 2000 К. Функції LTEC розраховувались як в площині, так і в позапланові напрямки. Крім того, закон Дулонга-Петі також був підтверджений, не проявляючи жодних неприродних явищ. В результаті розрахунків фаза  $Ti_6Si_2B$  повинна бути стійкішою порівняно з фазою  $Ti_3B_4$ .

**Ключові слова:** дослідження in initio, обчислення DFT, наближення VASP, інтерметалічна фаза, високотемпературні структурні програми.

**Aims of the article.** The main aim of this paper is to characterize the thermodynamic properties of the  $Ti_6Si_2B$  phase. Additional goal is to present LTEC curves with taking into account Grüneisen formalism. At the end final determination of whether the phase  $Ti_6Si_2B$  has potential in high temperature applications.

**The most recent scientific researches.** The thermodynamic studies over  $Ti_6Si_2B$  phase are made

by C. Colinet, J. C. Tedenac in 2011. Nowadays team of A. S. Ramos sheds new light on the electronic structure of this intermetallic phase in 2020. At present, new development perspectives have appeared.

**Problem statement.** Rietveld refinement of X-ray powder intensity data revealed a hexagonal crystal structure of  $Ti_6Si_2B$  [1]. Nowadays, intensive ab initio research is being carried out to predict the physical and chemical parameters of the structure [2]. This ter-

nary phase belongs to 189 (P – 6 2 m) space group with lattice parameters  $a = 0.68026$  nm and  $c = 0.33374$  nm obtained from high temperature X-ray diffraction at room temperature [3]. The Wyckoff positions of each atom are:  $Ti_1 = 3g$  ( $XTi_1, 0, 1/2$ ), where  $XTi_1 = 0.2418$ ;  $Ti_2 = 3f$  ( $XTi_2, 0, 0$ ) where  $XTi_2 = 0.5996$ ;  $B = 1a$  ( $0, 0, 0$ ) and  $Si = 2d$  ( $1/3, 2/3, 1/2$ ) (Fig. 1). The ternary  $Ti_6Si_2B$  phase forms from the liquid through the peritectic reaction:  $L + TiB + Ti_5Si_3 \leftrightarrow Ti_6Si_2B$ . RM-SiB (RM-refractory metal) alloys have been considered to high temperature structural applications due to their phenomenal physical, mechanical and chemical properties such as low thermal expansion anisotropy  $\alpha_c/\alpha_a \approx 1$  at room temperature [3], high mechanical strength (above 150 GPa) [4], high melting temperature (1473 K) [5], oxidation resistance (900 °C) [6] and relatively low density (4.3 g/cm<sup>3</sup>) [7]. Several studies have been recently carried out aiming at the use of metal-Si-B systems for high temperature structural applications [8-10]. In this sense, alloys which microstructure are formed by intermetallic phases in equilibrium with refractory metal or alloy could be developed [11]. However, informations concerning Ti-Si-B ternary system are very narrow. Only limited phase equilibria data are available in the literature. Most of the experimental informations concern the calculated isothermal sections at 727°C, 1250°C and 1600°C [12–14]. As part of the studies related to the Ti-Si-B systems, in this paper I present results focusing at thermodynamic properties of  $Ti_6Si_2B$ .

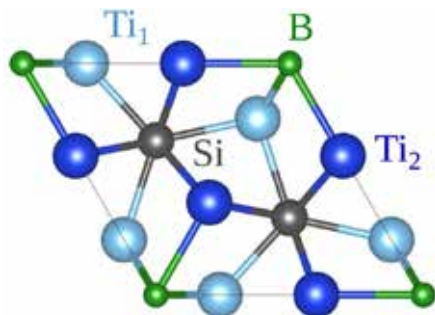


Figure 1. View of  $Ti_6Si_2B$  primitive cell along the  $c$  axis

Source: figure made by author

**Scientific analysis.** Ab initio calculations of thermodynamic properties of the hexagonal  $Ti_6Si_2B$  were performed within the density functional theory (DFT). The  $Ti(3d^34s^1)$ ,  $Si(3s^23p^2)$  and  $B(2s^22p^1)$  electrons were explicitly treated as valence electrons. The pseudopotential method with the generalized gradient approximation (GGA) parameterized by Perdew-Burke-Ernzerhof method (PBE) as implemented in the VASP code [15] was used to optimize geometry and atomic positions of the 54-atomic supercell. Atoms were represented by the projector-augmented wave pseudopotentials (PAWs) provided by VASP. A plane-wave expansion up to cutoff energy 420 eV was applied. The Brillouin zone of each super-cell was sampled using the  $5 \times 5 \times 10$  k-point mesh generated by the Monkhorst-Pack scheme. A combination of conjugate gradient energy minimization and a quasi-Newton force minimization was used to optimize geometry and the atomic positions of the supercells. During thermodynamic calculations, the lattice vectors of the super-cell were frozen at the GGA optimized value

and the atomic positions were relaxed until the Hellman-Feynmann (HF) forces acting on all atoms of the super-cell were smaller than  $10^{-6}$  eV/Å. Dynamical properties of the  $Ti_6Si_2B$  structure were calculated using the direct method [15–16] based on the forces calculated via the Hellmann-Feynman theorem. The nonvanishing Hellmann-Feynman (HF) forces acting on each atom in the given supercell are generated when a single atom is displaced from its equilibrium position. The HF forces were created by displacing crystallographically nonequivalent Ti, Si and B atoms from their equilibrium positions. The displacement amplitude of 0.03 Å was used. To minimize systematic error, both positive and negative displacements were applied. The total energy was converged down to  $10^{-8}$  eV/super-cell.

**Thermodynamic properties of the  $Ti_6Si_2B$ .** The thermodynamic properties of the  $Ti_6Si_2B$  structure were obtained within the quasiharmonic approximation and using the direct method [14], which uses the DFT calculated HF forces acting on all the atoms in a given supercell. Along with this approach a change of the crystal volume due to finite temperature is mapped with respect to change of the crystal volume at  $T = 0$  K. Thermodynamic functions are calculated using standard formulae for harmonic crystals. Anharmonic effects are, to some extent, taken into account by the volume dependence of the phonon frequencies. Phonon frequencies at constant volume are assumed to be independent of temperature. The relative change of the  $(q, j)$  mode frequency  $\omega(q, j)$  with volume  $V$  is usually described by the mode-specific Grüneisen parameter which is a dimensionless quantity defined as:

$$\gamma(k, j) = - \frac{\partial (\ln \omega(k, j))}{\partial \ln V} = - \frac{V}{\omega(k, j)} \frac{\partial \omega(k, j)}{\partial V} \quad (1)$$

The thermal Grüneisen parameter  $\gamma(T)$  can be obtained as the following average:

$$\gamma(T) = \frac{\sum_{k,j} \gamma(k, j) C_V(k, j)}{\sum_{k,j} C_V(k, j)} \quad (2)$$

where the contribution from each mode  $(q, j)$  is weighted by its contribution to the specific heat  $C_V(q, j)$ . The denominator of the above equation is equal to the lattice contribution to the heat capacity at constant volume and it takes on the following form:

$$C_V = k_B \sum_{k,j} \left( \frac{\hbar \omega(k, j)}{2k_B T} \right)^2 \frac{1}{\sinh^2(\hbar \omega(k, j)/2k_B T)} \quad (3)$$

where  $T$  is the temperature,  $k_B$  and  $\hbar$  denote the Boltzmann and Dirac constants respectively. One can also express  $C_V$  via the calculated phonon density of states  $g(\omega)$ . Hence, the equivalent form of equation (3) is given by:

$$C_V = N r k_B \int_0^\infty d\omega g(\omega) (\hbar/k_B T) \frac{\exp(\hbar \omega/k_B T)}{[\exp(\hbar \omega/k_B T) - 1]^2} \quad (4)$$

where  $N$  is the number of primitive unit cells and  $r$  stands for the number of degrees of freedom in the unit cell. In the quasiharmonic approximation the phonon density of states can be used to evaluate phonon-dependent thermodynamic quantities as a function of volume and temperature. In particular, the Helmholtz free energy of the material can be expressed in the following way:

$$F(V, T) = E(V) + F_{ph}(V, T) = E(V) + k_B T \cdot \int_0^\infty g(\omega) \ln \left[ 2 \sinh \left( \frac{\hbar \omega}{2k_B T} \right) \right] \quad (5)$$

where  $E(V)$  is the energy of the motionless lattice obtained directly from ab initio calculations, while  $F_{ph}(V, T)$  denotes the vibrational free energy of a harmonic system. The term  $F_{ph}(V, T)$  includes the vibrational zero-point energy which remains finite for  $T \rightarrow 0$ . Any purely electronic contribution is neglected. One has to note that only  $F_{ph}(V, T)$  depends explicitly on temperature. At the given temperature  $T$ , the equilibrium volume follows from a minimization of  $F(V, T)$  with respect to volume  $V$ . The calculated  $F(V, T)$  can be used to study thermal properties and thermodynamic parameters of the crystal. The volume thermal expansion coefficient is defined as:

$$\alpha_V(T) = \frac{1}{V} \left( \frac{\partial V}{\partial T} \right)_P \quad (6)$$

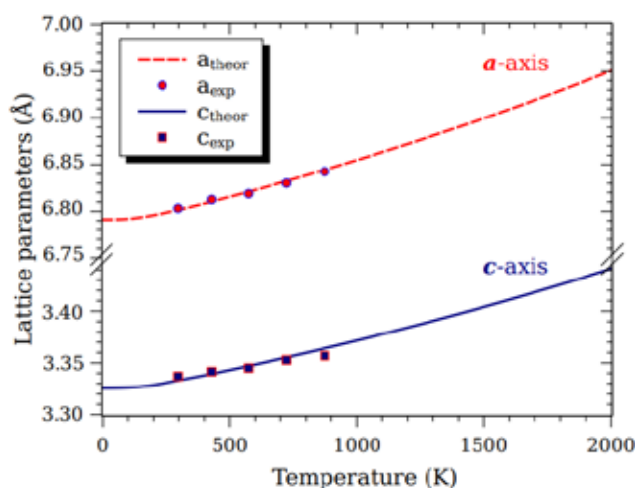


**Figure 2.** The a- and c-axis lattice constants of  $Ti_6Si_2B$  structure. The lines represent ab initio calculated data, points refer to experimental high temperature x-ray diffraction results [3]

Source: figure made by author

In the quasiharmonic approximation the quantities:  $\alpha_V$ ,  $C_V$ ,  $\gamma$  and the isothermal bulk modulus  $B_T = V(\partial^2 F(V, T)/\partial V^2)_T$  are connected by the Grüneisen relation:

$$\gamma(T) = \frac{V \alpha_V B_T}{C_V} \quad (7)$$

Thermal expansivity of a crystal leads to the difference between the heat capacity at constant pressure  $C_p$  and the heat capacity at constant volume  $C_V$ , which is given in the quasiharmonic approach by the following expression:

$$C_p - C_V = \alpha_V^2(T) B T V \quad (8)$$

The heat capacity  $C_V$  follows the Debye model and approaches the Dulong-Petit limit at high temperatures, while  $C_p$  increases linearly with  $T$  at high temperatures.

### Results and discussion

#### Structural properties of $Ti_6Si_2B$ – phase

The computed with the use of (5) relation  $F(V, T)$  values could be useful to determine lattice constants of the crystal. These structural parameters

were obtained as the derivative of the changing cell volume with respect to temperature according with the relation for volume of hexagonal structure  $V = a^2 c \cdot \sin(60^\circ)$ . The calculated structural parameters of the  $Ti_6Si_2B$  are presented at (Fig. 2). The received curves are in good agreement with high temperature x-ray experimental measurements [3].

#### Elastic properties of $Ti_6Si_2B$ crystal

The optimized structure was used to calculate elastic constants of  $Ti_6Si_2B$  crystal. The number of elastic constants needed to describe the elastic response of a crystal depends on its symmetry. The elastic tensor of the hexagonal system is determined by five independent elements i.e.  $C_{11}$ ,  $C_{12}$ ,  $C_{13}$ ,  $C_{33}$  and  $C_{44}$ . What is more elastic tensor in this case is symmetric  $C_{ij} = C_{ji}$  and there are some symmetry relations:  $C_{11} = C_{22}$ ,  $C_{13} = C_{23}$ ,  $C_{44} = C_{55}$  and  $C_{66} = 1/2(C_{11} - C_{12})$ . The computed components of the elastic tensor for  $Ti_6Si_2B$  are given in table 1. By the inversion of elastic tensor we are receiving the compliance tensor which elements  $S_{ij} = C^{-1}_{ij}$  can be used to derive the linear compressibilities along the principal axes of the crystal. For hexagonal structures symmetry of elements and symmetry relations of compliance tensor are exact the same as for elastic tensor. The calculated components of the compliance tensor for  $Ti_6Si_2B$  are given in table 2.

Table 1  
Elastic constants (in GPa) of  $Ti_6Si_2B$

$C_{11}$	$C_{12}$	$C_{13}$	$C_{33}$	$C_{44}$
303	78	87	249	114

Source: table made by author

Table 2  
Compliance constants (in  $10^{-12} \text{ GPa}^{-1}$ ) of  $Ti_6Si_2B$

$S_{11}$	$S_{12}$	$S_{13}$	$S_{33}$	$S_{44}$
3.778	-0.650	-1.098	4.787	8.775

Source: table made by author

The linear compressibilities can be easily derived from the compliance tensor  $S_{ij}$ . Full expressions for an arbitrary direction in a triclinic crystal can be found in [17], along the coordinate axes they are:

$$K_a = \sum_{j=1}^3 S_{1j} \quad K_b = \sum_{j=1}^3 S_{2j} \quad K_c = \sum_{j=1}^3 S_{3j} \quad (9)$$

Hence, the bulk compressibility is expressed as [17]:

$$K = \sum_{i=1}^3 \sum_{j=1}^3 S_{ij} = K_a + K_b + K_c \quad (10)$$

There are several different schemes which enable to obtain the Reuss averaged bulk/shear moduli. By an assumption of a homogeneous stress we can use a special averaging for the individual  $S_{ij}$  expressed as [17]:

$$B_R = \frac{1}{K} = \frac{1}{S_{11} + S_{22} + S_{33} + 2(S_{12} + S_{13} + S_{23})} \quad (11)$$

$$G_R = \frac{15}{4(S_d) - 4(S_{12} + S_{13} + S_{23}) + 3(S_{44} + S_{55} + S_{66})} \quad (12)$$

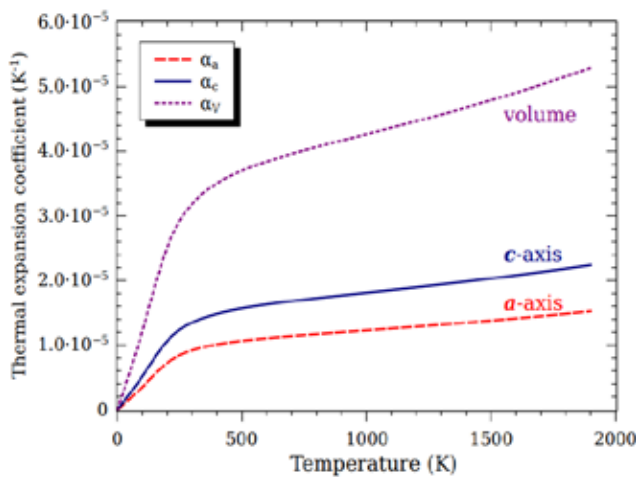


Figure 3. Computed thermal expansion coefficients along with a- and c-axis with total volumetric thermal expansion parameter

Source: figure made by author

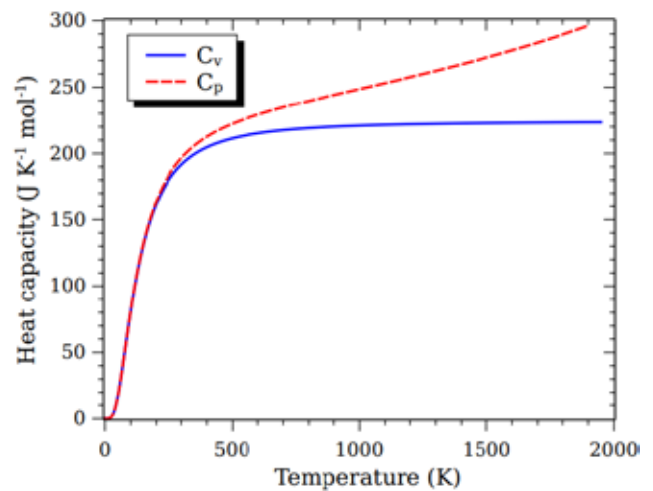


Figure 4. Temperature dependence of the constant pressure and volume heat capacity  $C_p$  and  $C_v$ , respectively

Source: figure made by author

where  $S_d = S_{11} + S_{22} + S_{33}$  indicates the sum of the diagonal elements of compliance tensor. Table 3 shows the resultant bulk and shear moduli as well as the linear compressibilities along the principal axes of  $Ti_6Si_2B$  crystal. The above computed quantities can be applied to calculate the Young's modulus  $E$  and Poisson's ratio  $\nu$  for an isotropic material by the following relations (13) and (14):

$$E = \frac{9B_R G_R}{3B_R + G_R} \quad (13)$$

Table 3  
Linear compressibilities, bulk  $B_R$  and shear  $G_R$  moduli of  $Ti_6Si_2B$ . Compressibilities and moduli are given in  $10^{-12} \text{ GPa}^{-1}$  and  $\text{GPa}$ , respectively

$K_a$	$K_b$	$K_c$	$B_R$	$G_R$
2.030	2.034	2.587	150.377	109.055

Source: table made by author

$$\nu = \frac{3B_R - 2G_R}{2(3B_R + G_R)} \quad (14)$$

Table 4 shows the final Young's modulus and Poisson's ratio. The ratio  $B_R/G_R$  for the polycrystalline phases is a factor indicating the ductility or brittleness of a material and the critical value which separates ductile and brittle materials is about 1.75 [18]. According to this criterion,  $Ti_6Si_2B$  is predicted to be brittle  $B_R/G_R = 1.379$ .

Table 4  
Young's modulus, Poisson's ratio,  $B_R/G_R$  and  $E/G_R$  of  $Ti_6Si_2B$ . Moduli and appropriate ratios are given in  $\text{GPa}$  and a.u., respectively

$E$	$\nu$	$B_R/G_R$	$E/G_R$
263.474	0.208	1.379	2.416

Source: table made by author

### Thermal properties of $Ti_6Si_2B$ supercell

Linear thermal expansion coefficient LTEC measures the fractional change in size per degree change in temperature at a constant pressure. To calculate total volumetric thermal expansion parameter it is convenient to use  $\alpha_v = 2\alpha_a + \alpha_c$  expression, where  $\alpha_a$  and  $\alpha_c$  represent thermal expansion coefficients along a- and c-axes, respectively. It is visible positive trend of computed dependences (Figure 3), the thermal expansion along the c axis is higher than along the a axis.

### Heat capacity of $Ti_6Si_2B$ structure

Temperature dependences of molar heat capacity at constant pressure and at constant volume were calculated with the use of (8) expression (Fig. 4). Solid curve represents determined  $C_v$  values according to the harmonic approximation. Dashed curve denote  $C_p$  values obtained with the quasiharmonic approximation. The term  $\alpha_v^2(T)BVT$  accounts for the lattice anharmonicity. It is relevant at higher temperatures where the difference between  $C_v$  and  $C_p$  can be significant. Heat capacity  $C_v$  was computed based on ab initio considerations (3), afterwards by (8) relation heat capacity  $C_p$  was derived. The received curves are in good agreement with Dulong-Petit law predictions for solid systems.

**Conclusions.** The structural and thermodynamic properties of  $Ti_6Si_2B$  crystal have been studied by the quasiharmonic approximation with density functional theory DFT. The calculated thermodynamic properties of  $Ti_6Si_2B$  - phase stay in acceptable agreement with the available experimental data.

**Acknowledgements.** This research has been supported by the EU Project POWR.03.02.00-00-I004/16 and the statutory funds of AGH University of Science and Technology Department of Materials Science and Ceramics AGH.

**References:**

1. A. S. Ramos, C. A. Nunes, G. Rodrigues, P. A. Suzuki, G. C. Coelho, A. Grytsiv, P. Rogl, *Intermetallics* 12 (2004), p. 487–491.
2. G. Kresse and J. Furthmuller, *Phys. Rev. B* 54 (1996), p. 169.
3. G. Rodrigues, C. A. Nunes, P. A. Suzuki, G. C. Coelho, *Intermetallics* 14 (2006), p. 236–240.
4. A. Potekaev, A. Klopotov, Yu. Ivanov, O. Volokitin, *Russian Physics Journal* 56 (2013).
5. S. O. Firstov, I. D. Horna, K. O. Horpenko, M. D. Beha, O. Yu. Koval, A. V. Kotko, *Materials Science* 44 (2008), p. 342–351.
6. E. C. T. Ramos, G. Silva, A. S. Ramos, C. A. Nunes, C. A. R. P. Baptista, *Materials Science and Engineering A363* (2003), p. 297–306.
7. B. B. Fernandes, M. Ueda, G. S. Savonov, C. M. Neto, A. S. Ramos, *IEEE Transactions on Plasma Science* 39, 11 (2011), p. 3061–3066.
8. K. Ito, M. Kumagai, T. Hayashi, M. Yamaguchi, *Scripta Mater* 49(4) (2003), p. 285.
9. D. M. Pinto-Junior, C. A. Nunes, G. C. Coelho, F. Ferreira, *Intermetallics* 11(3) (2003).
10. J. H. Schneibel, M. J. Kramer, D. S. Easton, *Scripta Materialia* 46(3) (2002), p. 217.
11. G. Silva, E. C. T. Ramos, D. M. Silverio, A. S. Ramos, K. R. Cardoso, C. A. Nunes, *Journal of Metastable and Nanocrystalline Materials* 20-21 (2004), p. 145–150.
12. J. S. Park, R. Sakidja, J. H. Perepezko, *Scripta Materialia* 46(11) (2002), p. 765. K. Maex, G. Ghosh, L. Delaey, V. Probst, *J Mater Res* 4(5) (1989), p. 1209.
13. Y. Yang, Y. A. Chang, L. Tan, *Intermetallics* 13 (2005), p. 1110–1115.
14. K. Parlinski, Z. Q. Li, Y. Kawazoe, *Phys. Rev. Lett.* 78 (1997).
15. K. Parlinski, *Software PHONON* (2008) Krakow, Poland.
16. A. R. Oganov, J. P. Brodholt, G. D. Price, *EMU Notes in Mineralogy* 4 (2002), p. 83–170.
17. S. F. Pugh, *Phil. Mag.* 45 (1954), p. 823.